Filtering Push–Pull Power Amplifier Based on Multifunctional Impedance Matching Network

Gaoya Dong, Xiaolong Yang, *Member, IEEE*, Yunnan Fang, and Manos M. Tentzeris, *Fellow, IEEE*

***Abstract*— A filtering push–pull power amplifier (PPPA) is presented based on the multifunctional impedance matching network (MIMN), which is constructed by coupled lines and open-circuited transmission lines. Due to the symmetry of designed MIMN, the even-and odd-mode method is employed to analyze the operating mechanisms, which reveal that designed MIMN can achieve high common mode suppression under the even-mode excitation, while provide good impedance transformation and filtering response under the odd-mode excitation. Finally, a filtering PPPA based on the MIMN is designed as well as measured, and the measured operating frequencies are ranging from 1.85 to 2.03 GHz. The measured maximum gain and peak power-added efficiency are 13.9 dB and 57.8%, while the measured upper stopband extends to $4.1f_0$ with the suppression level of 20 dB.**

***Index Terms*— Compact size, filtering response, push–pull power amplifier (PPPA), wide upper stopband.**

I. Introduction

POWER amplifiers (PAs) can amplify the signals, thus playing important roles in the modern wireless communication systems [1]–[3]. In the conventional radio frequency front ends, the PAs are usually connected with the bandpass filters (BPFs) to select the wanted signals and suppress the out-of-band interferences [4]. The inherent insertion losses in BPFs and the connection losses due to the mismatch between the components are unavoidable. To deal with these problems, the co-design of BPF and PA is imperative and indispensable.

The co-design method of BPF and single-end PA are introduced in [5], [6]. A BPF with the functions of filtering response and impedance transformation is utilized in [5] as the output matching network, presenting a class-AB PA integrated with filtering response. In [6], a class-F filtering PA is proposed by adopting the hybrid cavity-microstrip filtering circuit, which not only to realize output impedance matching but also to provide high-selectivity bandpass response.

Recently, push–pull power amplifier (PPPA) have attracted a lot of attentions due to the advantages of high efficiency and linearity. The main difficulty in designing PPPA is to realize the conversion between unbalanced and balanced, which are already achieved by uniplanar microstrip line baluns [7]–[10], rat-race microstrip baluns [3] as well as broadband Marchand baluns [11], and the impedance transformation performances in the uniplanar baluns have been discussed. However, the baluns introduced in [3], [7]–[11] cannot provide filtering responses and out-of-band suppression performances. Thus, the main design challenge of filtering PPPA is to construct the multifunctional circuit, which could realize impedance transformation, 180° phase difference, and filtering response simultaneously. In [12], a novel filtering PPPA is introduced based on the unbalanced to balanced impedance transformer, which is composed of two different C-type line resonators. Moreover, in the designed impedance transformer [12], the filtering response is obtained based on the specific coupling between two C-type line resonators, while the 180° phase difference is achieved by adopting $\lambda_g/2$ transmission lines. In [13], a bandpass PPPA based on substrate integrated waveguide (SIW) filtering balun power divider is proposed. The filtering characteristic is realized based on the complementary split rings resonators (CSRRs) defected in the balun, while the 180° phase difference power division is achieved by utilizing the inherent middle metal plane of the SIW balun.

In this letter, a filtering PPPA with low loss, high efficiency, and improved harmonic suppression performance is proposed based on the designed multifunctional impedance matching networks (MIMNs). Due to the symmetry of designed MIMN, the even- and odd-mode method is adopted to analyze the operating mechanisms. Specifically, the impedance matching in designed MIMN can be adjusted by tuning the capacitances and the characteristic impedances of transmission lines, while the out-of-band suppression can be improved by introducing transmission zeros (TZs) in the upper stopband. Finally, a compact filtering PPPA based on the designed MIMN has been simulated, fabricated and measured to validate the presented idea.

II. Push–Pull Power Amplifier Design

The schematic of designed filtering PPPA is illustrated in Fig. 1, in which a filtering unbalanced to balanced balun (transformation from 50 to 20 Ω) is adopted as the input impedance transformer, and a filtering balanced to unbalanced balun (transformation from 20 to 50 Ω) is employed as the output impedance transformer. The stability networks are

Manuscript received October 30, 2021; accepted December 15, 2021. Date of publication January 10, 2022; date of current version May 10, 2022. This work was supported in part by the Fundamental Research Funds for the Central Universities under Grant 06116163 and in part by the Post-Doctor Research Foundation of the Shunde Graduate School of University of Science and Technology Beijing under Grant 2021BH004. *(Corresponding author: Gaoya Dong.)*

Gaoya Dong is with the School of Computer and Communication Engineering, University of Science and Technology Beijing, Beijing 100083, China, and also with the Shunde Graduate School, University of Science and Technology Beijing, Foshan, Guangdong 528399, China (e-mail: gaoyadong@ustb.edu.cn).

Xiaolong Yang is with the School of Computer and Communication Engineering, University of Science and Technology Beijing, Beijing 100083, China.

Yunnan Fang and Manos M. Tentzeris are with the School of Electrical Computer Engineering, Georgia Institute of Technology, Atlanta, GA 30332 USA.

Color versions of one or more figures in this letter are available at https://doi.org/10.1109/LMWC.2021.3136718.

Digital Object Identifier 10.1109/LMWC.2021.3136718

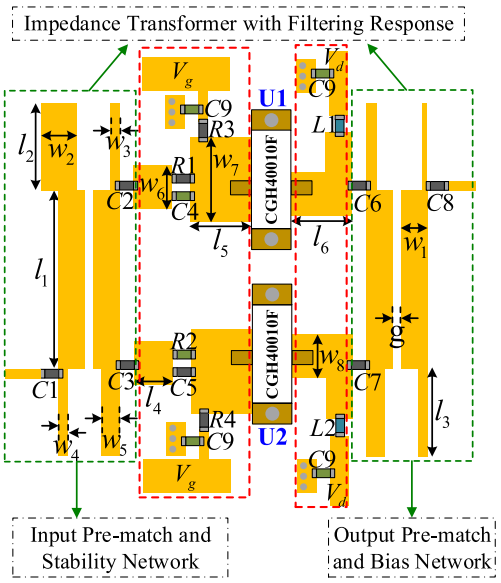

Fig. 1. Topology of the filtering PPPA.

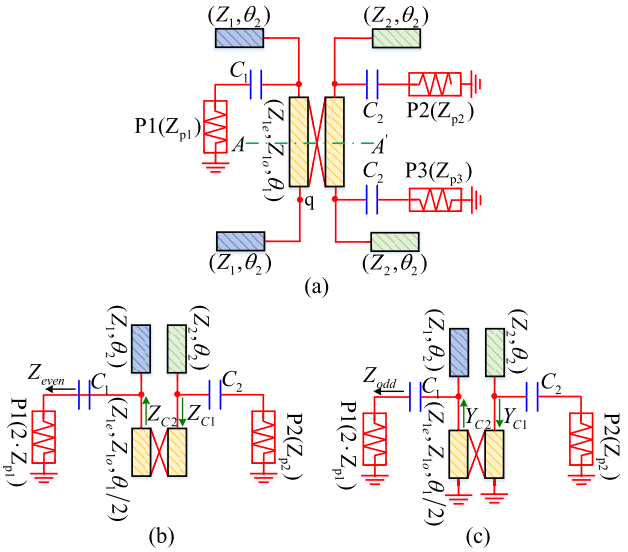

Fig. 2. (a) Schematic. (b) Even-mode equivalent circuit. (c) Odd-mode equivalent circuit of designed MIMN.

constructed by RC networks (R_1, C_4, and R_2, C_5) and gate biasing resistors (R_3 and R_4), while the bias networks are composed of two lumped inductors ($L1$ and $L2$). Moreover, two power transistors (CGH40010F) are adopted to amplify the signals, while the gate voltage (V_{GS}) and drain voltage (V_{DS}) are applied on four solder pads.

The schematic of designed MIMN is exhibited in Fig. 2, which can be considered as a four-port network with the fourth port being opened at node "q." The designed MIMN consists of one core coupled line (Z_{1e}, Z_{1o}, θ_1), four open-circuited TLs [(Z_1, θ_2), (Z_2, θ_2)], and three capacitances (C_1, C_2, C_3), while the θ_1 and θ_2 are selected as 90° and 45 at f_0 ($\theta_1 = 2\theta_2$). Define $Z_C = (Z_{1e} \times Z_{1o})^{1/2}$ and $k = (Z_{1e} - Z_{1o})/(Z_{1e} + Z_{1o})$. Due to the symmetry of designed MIMN, the corresponding even- and odd-mode equivalent circuit can be derived and shown in Fig. 2(a) and (b), respectively.

According to [14], [15], the governing equations for the balun should satisfy (1) and (2), and the impedance matrix of coupled line has been analyzed in [16] and shown in (3). In addition, the terminal condition of open-circuited coupled lines (Z_{1e}, Z_{1o}, $\theta_1/2$) can be expressed as (4) from Fig. 2(b). By submitting (4) into (3), the impedance transformation characteristic of the open-circuited coupled line can be obtained and exhibited in (5). Then, based on Fig. 2(b) and transmission line theory, the expressions of the even-mode input impedance (Z_{even}) in the port 1 can be deduced as (6). Similarly, the expression of odd-mode input impedance (Z_{odd}) in the port 1 an be derived and exhibited in (7) from Fig. 2(c). To satisfy (1), the condition can be derived as formula (8) by making sure the imaginary part of Z_{even} equals 0, which provides the guidance for the initial value selections of C_2 and θ_2. In a special case, under even-mode excitation, the value of Y_{C2} tends to 0 at $2n f_0$ ($n \in 1, 2, \ldots, N$), and the Z_{odd} is a pure imaginary number. Thus, under odd-mode excitation, the TZs are introduced at $2n f_0$, which is helpful to improve the out-of-band suppression performance

$$T_{\text{even}} = 0 \tag{1}$$

$$Z_{\text{odd}} = 2 \cdot Z_{p1} \tag{2}$$

$$\begin{bmatrix} V_1 \\ V_2 \\ V_3 \\ V_4 \end{bmatrix} = \begin{bmatrix} Z_{1a} & Z_{2a} & Z_{3a} & Z_{4a} \\ Z_{2a} & Z_{1a} & Z_{4a} & Z_{3a} \\ Z_{3a} & Z_{4a} & Z_{1a} & Z_{2a} \\ Z_{4a} & Z_{3a} & Z_{2a} & Z_{1a} \end{bmatrix} \begin{bmatrix} I_1 \\ I_2 \\ I_3 \\ I_4 \end{bmatrix} \tag{3}$$

where

$$Z_{1a} = \frac{-j \cdot Z_C \cdot \cot(\theta_1/2)}{1-k^2}, \quad Z_{2a} = \frac{-j \cdot Z_C \cdot k \cdot \cot(\theta_1/2)}{1-k^2}$$
$$Z_{3a} = \frac{-j \cdot Z_C \cdot k \cdot \csc(\theta_1/2)}{1-k^2}, \quad Z_{4a} = \frac{-j \cdot Z_C \cdot \csc(\theta_1/2)}{1-k^2}$$
$$V_1 = I_1 \cdot Z_{C1}, \quad -V_2 = I_2 \cdot Z_{C2}, \quad I_3 = 0, \quad I_4 = 0 \tag{4}$$

$$Z_{C2} = \text{conj}\left(-\frac{Z_{2a}^2 - Z_{1a}^2 + Z_{C1} \cdot Z_{1a}}{Z_{C1} - Z_{1a}}\right) \tag{5}$$

where

$$Z_{C1} = \text{conj}\left(1 \Big/ \left(\frac{1}{Z_{p2} + 1/j \cdot \omega \cdot C_2} + \frac{j \cdot \tan(\theta_2 \cdot f_x/f_0)}{Z_2}\right)\right)$$

$$Z_{\text{even}} = \frac{1}{1/Z_{C2} + j \cdot \tan(\theta_2 \cdot f_x/f_0)/Z_1} + \frac{1}{j \cdot \omega \cdot C_1} \tag{6}$$

$$Z_{\text{odd}} = \frac{1}{Y_{C2} + j \cdot \tan(\theta_2 \cdot f_x/f_0)/Z_1} + \frac{1}{j \cdot \omega \cdot C_1} \tag{7}$$

where

$$Y_{C2} = \text{conj}\left(-\frac{Y_{2a}^2 - Y_{1a}^2 + Y_{C1} \cdot Y_{1a}}{Y_{C1} - Y_{1a}}\right)$$
$$Y_{C1} = \text{conj}\left(\frac{1}{Z_{p2} + 1/j \cdot \omega \cdot C_2} + \frac{j \cdot \tan(\theta_2 \cdot f_x/f_0)}{Z_2}\right)$$
$$Y_{1a} = -\frac{j \cdot Y_C \cdot \cot(\theta_1/2)}{1-k^2}, \quad Y_{2a} = -\frac{j \cdot Y_C \cdot k \cdot \cot(\theta_1/2)}{1-k^2}$$
$$Y_{3a} = -\frac{j \cdot Y_C \cdot k \cdot \csc(\theta_1/2)}{1-k^2}, \quad Y_{4a} = -\frac{j \cdot Y_C \cdot \csc(\theta_1/2)}{1-k^2}$$
$$\times C_2 \cdot \omega \cdot Z_{p2} \cdot \cos\theta_2 + \sin\theta_2 = 1. \tag{8}$$

Based on the analysis above, the even- and odd-mode input impedances (Z_{even}, Z_{odd}) in the port 1 can be calculated from (6) and (7). Then, Z_{even} and Z_{odd} against frequencies with

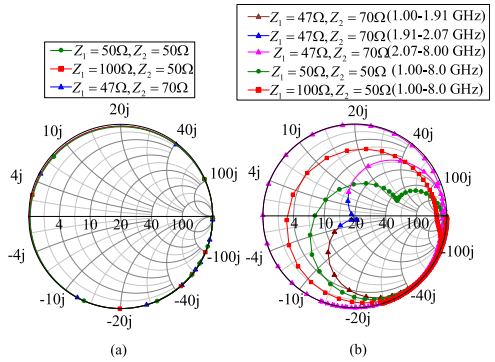

Fig. 3. (a) Even-mode and (b) odd-mode input impedances of port 1 against frequencies with different values of Z_1 and Z_2 (normalized to 20 Ω).

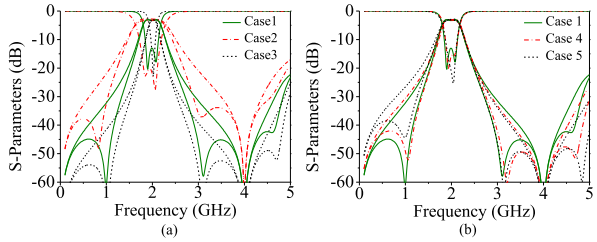

Fig. 4. Frequency responses of the designed MIMN (a) with different passband bandwidths and (b) with different impedance matching.

TABLE I
DETAILED PARAMETER VALUES OF MIMN UNDER DIFFERENT CASES

Case	Impedance transmission	Z_c (Ω)	Z_1 (Ω)	Z_2 (Ω)	Z_3 (Ω)	C_1 (pF)	C_2 (pF)	k
Case 1	50 Ω to 50 Ω	36	47	70	43	2.4	1.2	0.22
Case 2	50 Ω to 50 Ω	27	60	70	19	3.2	2.5	0.35
Case 3	50 Ω to 50 Ω	36	47	70	43	2.4	1.2	0.12
Case 4	50 Ω to 20 Ω	41	33	70	72	2.2	1.0	0.22
Case 5	50 Ω to 100 Ω	33	53	70	80	1.5	1.8	0.22

different values of Z_1 and Z_2 are plotted in Fig. 3. As observed from Fig. 3(a), ranging from 0.1 to 10.0 GHz, the real parts of Z_{even} almost remain zero with different values of Z_1 and Z_2 and result in high even-mode suppression performance. It is seen from Fig. 3(b) that Z_{odd} could be adjusted by tuning the values of Z_1 and Z_2. Specifically, $Z_1 = 47\ \Omega$ and $Z_2 = 70\ \Omega$, the Z_{odd} is matched to 20 Ω from 1.91 to 2.07 GHz, and Z_{odd} moves away from 20 Ω during 1.00–1.90 GHz and 2.08–8.00 Hz, resulting in good-selectivity bandpass response.

The frequency responses of designed MIMN with different parameter values are depicted in Fig. 4, and the corresponding parameter values are given in Table. I. As observed form Fig. 4(a), the passband bandwidths in the designed MIMN can be controlled by tuning the value of "k", and bigger "k" will result in wider passband bandwidth. It is seen from Fig. 4(b) that impedance transformation performances in the MIMN can be adjusted by changing the capacitances and characteristic impedances of transmission lines. Accordingly, the passband bandwidth and impedance transformation performance in the designed MIMN can be independently controlled.

III. IMPLEMENTATION AND MEASUREMENT

To verify the presented idea, a filtering PPPA with wide stopband suppression is fabricated on the substrate with the dielectric of 3.66 and the thickness of 20 mil. Moreover, the photograph and detailed dimensions of designed filtering PPPA are given in Fig. 5.

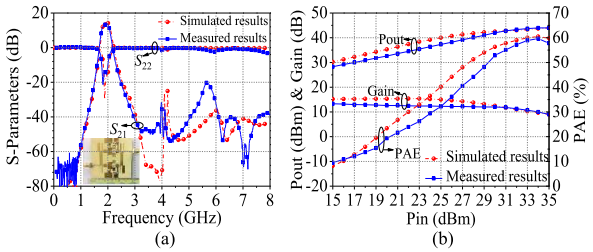

Fig. 5. (a) Simulated and measured S-parameters. (b) Simulated and measured P_{out}, gains and PAEs. The detailed values of the presented filtering PPPA: $l_1 = 20$ mm, $l_2 = 11$ mm, $l_3 = 11$ mm, $l_4 = 4$ mm, $l_5 = 7$ mm, $l_6 = 5$ mm, $W_1 = 2$ mm, $W_2 = 3.5$ mm, $W_3 = 1$ mm, $W_4 = 0.5$ mm, $W_5 = 1$ mm, $W_6 = 5$ mm, $W_7 = 10$ mm, $W_8 = 4$ mm, $g = 0.2$ mm, $C_1 = 1.2$ pF, $C_2 = 1.3$ pF, $C_3 = 1.3$ pF, $C_4 = 3.0$ pF, $C_5 = 3.0$ pF, $C_6 = 1.3$ pF, $C_7 = 1.3$ pF, $C_8 = 1.2$ pF, $C_9 = 3.0$ pF, $R_1 = 12\ \Omega$, $R_2 = 12\ \Omega$, $R_3 = 30\ \Omega$, $R_4 = 30\ \Omega$, $L_1 = 6.8$ nH, $L_2 = 6.8$ nH.

TABLE II
COMPARISONS WITH SOME PRIOR PAS

Ref.	Fre.	Type	FBW	Pout (dBm)	PAE (%)	Gain (dB)	Filtering response	Size (λ_g^2)	Rejection Perfomance
[4]	1.50	class-AB	133.3%	43.0	63.0%	18.0	N	0.22×0.22	N
[5]	2.60	class-AB	3.8%	42.5	46.3%	14.4	Y	1.01×1.30	$2.3f_0(\geq 20dB)$
[6]	2.40	class-F	5.4%	40.0	70.9%	18.2	Y	0.89×0.32	$1.7f_0(\geq 30dB)$
[12]	2.40	push-pull	8.6%	42.0	57.8%	12.0	Y	/	$2.9f_0(> 14dB)$
[13]	5.50	push-pull	3.6%	38.5	48.7%	12.5	Y	2.12×1.18	$1.4f_0(> 40dB)$
This work	1.94	push-pull	9.3%	44.0	57.8%	13.9	Y	0.39×0.51	$4.0f_0(> 20dB)$

Under small-signal excitation, the simulated and measured results of designed filtering PPPA are plotted in the Fig. 5(a). Accordingly, the measured maximum gain is 13.9 dB at 1.96 GHz, while the measured 1-dB gain bandwidth is ranging from 1.85 to 2.03 GHz. Additionally, the measured out-of-band suppression level extends to 4.1 f_0 with the rejection level of 20 dB. Fig. 5(b) demonstrates the simulated and measured gain, output power (P_{out}), and power added efficiency (PAE) at 2.0 GHz with the input power ranging from 15 to 35 dBm. Moreover, the drain and gate voltages are selected as 28 and −2.0 V, respectively. According to Fig. 5(b), the measured maximum output power is 44 dBm with the input power of 35 dBm, and the peak PAE reaches to 57.8% when the input power is chosen as 34 dBm. The measured maximum gain is 13.3 dB with the input power of 15 dBm.

The performance comparisons between designed filtering PPPA and other similar works are exhibited in Table. II. Accordingly, the filtering PPPA presented in this letter has the advantages of compact size, wide upper stopband rejection, high efficiency, and P_{out}.

IV. CONCLUSION

In this letter, a novel design method for the filtering PPPA has been presented based on the MIMN, which could realize impedance transformation, balanced and unbalanced conversions, filtering response, and harmonic suppression simultaneously. Moreover, the passband bandwidth and impedance transmission in the MIMN can be controlled independently. The implemented filtering PA has shown both high-selectivity bandpass response and excellent power amplification, which is suitable for practical engineering application.

REFERENCES

[1] R. M. Smith, J. Lees, P. J. Tasker, J. Benedikt, and S. C. Cripps, "A novel formulation for high efficiency modes in push-pull power amplifiers using transmission line baluns," *IEEE Microw. Wireless Compon. Lett.*, vol. 22, no. 5, pp. 257–259, May 2012.

[2] Z. Wang, S. Gao, F. Nasri, and C.-W. Park, "High power added efficiency power amplifier with harmonic controlled by UWB filter with notched band at 6.42 GHz," in *Proc. WAMICON Conf.*, Apr. 2011, pp. 1–4.

[3] J. Park, C. Yoo, W. Kang, D. Kim, J. Yook, and W. S. Lee, "GaN HEMT based high efficiency push-pull inverse class-F power amplifier using chip-on-board technique," in *Proc. Asia–Pacific Microw. Conf.*, Dec. 2011, pp. 522–525.

[4] M. K. Roy, "Distortion cancellation performance of miniature delay filters for feed-forward linear power amplifiers," *IEEE Trans. Ultrason., Ferroelectr., Freq. Control*, vol. 49, no. 11, pp. 1592–1595, Nov. 2002.

[5] Y. C. Li, K. C. Wu, and Q. Xue, "Power amplifier integrated with bandpass filter for long term evolution application," *IEEE Microw. Wireless Compon. Lett.*, vol. 23, no. 8, pp. 424–426, Aug. 2013.

[6] Q. Y. Guo, X. Y. Zhang, J.-X. Xu, Y. C. Li, and Q. Xue, "Bandpass class-F power amplifier based on multifunction hybrid cavity–microstrip filter," *IEEE Trans. Circuits Syst. II, Exp. Briefs*, vol. 64, no. 7, pp. 742–746, Jul. 2017.

[7] M. H. Maktoomi, M. Zhou, H. Ren, Y. Gu, and B. Arigong, "A complex load matched microstrip balun," in *IEEE MTT-S Int. Microw. Symp. Dig.*, Jun. 2019, pp. 822–825.

[8] M. Zhou, H. Ren, and B. Arigong, "A novel microstrip line balun with transparent port impedance and flexible open arm structure," *IEEE Microw. Wireless Compon. Lett.*, vol. 30, no. 2, pp. 160–163, Feb. 2020.

[9] M. Zhou, H. Ren, Y. Gu, Y. Jin, and B. Arigong, "A novel uniplanar balun with transparent termination impedance," *IEEE Microw. Wireless Compon. Lett.*, vol. 29, no. 9, pp. 589–591, Sep. 2019.

[10] M. H. Maktoomi, H. Ren, M. N. Marbell, V. Klein, R. Wilson, and B. Arigong, "A wideband isolated real-to-complex impedance transforming uniplanar microstrip line balun for push–pull power amplifier," *IEEE Trans. Microw. Theory Techn.*, vol. 68, no. 11, pp. 4560–4569, Nov. 2020.

[11] J. J. Yan, Y. P. Hong, S. Shinjo, K. Mukai, and P. M. Asbeck, "Broadband high PAE GaN push-pull power amplifier for 500 MHz to 2.5 GHz operation," in *IEEE MTT-S Int. Microw. Symp. Dig.*, Jun. 2013, pp. 1–3.

[12] B. Zhang, G. Y. Dong, and Y. A. Liu, "Filtering push–pull power amplifier based on novel impedance transformers," *Electron. Lett.*, vol. 52, no. 17, pp. 1467–1469, Aug. 2016.

[13] W. Feng, Y. Shi, X. Y. Zhou, X. Shen, and W. Che, "A bandpass push–pull high power amplifier based on SIW filtering balun power divider," *IEEE Trans. Plasma Sci.*, vol. 47, no. 9, pp. 4281–4286, Sep. 2019.

[14] K. S. Ang, Y. C. Leong, and C. H. Lee, "Analysis and design of miniaturized lumped-distributed impedance-transforming baluns," *IEEE Trans. Microw. Theory Techn.*, vol. 51, no. 3, pp. 1009–1017, Mar. 2003.

[15] M. Zhou, J. Shao, B. Arigong, H. Ren, J. Ding, and H. Zhang, "Design of microwave baluns with flexible structures," *IEEE Microw. Wireless Compon. Lett.*, vol. 24, no. 10, pp. 695–697, Oct. 2014.

[16] G. I. Zysman and A. K. Johnson, "Coupled transmission line networks in an inhomogeneous dielectric medium," *IEEE Trans. Microw. Theory Techn.*, vol. MTT-17, no. 10, pp. 753–759, Oct. 1969.